

CrystEngComm

Accepted Manuscript



This is an *Accepted Manuscript*, which has been through the Royal Society of Chemistry peer review process and has been accepted for publication.

Accepted Manuscripts are published online shortly after acceptance, before technical editing, formatting and proof reading. Using this free service, authors can make their results available to the community, in citable form, before we publish the edited article. We will replace this *Accepted Manuscript* with the edited and formatted *Advance Article* as soon as it is available.

You can find more information about *Accepted Manuscripts* in the [Information for Authors](#).

Please note that technical editing may introduce minor changes to the text and/or graphics, which may alter content. The journal's standard [Terms & Conditions](#) and the [Ethical guidelines](#) still apply. In no event shall the Royal Society of Chemistry be held responsible for any errors or omissions in this *Accepted Manuscript* or any consequences arising from the use of any information it contains.

COMMUNICATION

Polymorphism and the influence of crystal structure on the luminescence of the optoelectronic material 4,4'-bis(9-carbazolyl)biphenyl

wwwCite this: DOI:
10.1039/x0xx00000x

Received 00th January 2012,
Accepted 00th January 2012

DOI: 10.1039/x0xx00000x

www.rsc.org/

Cody J. Gleason^a, Jordan M. Cox^a, Ian M. Walton^a, and Jason B. Benedict^{a,*}

Three polymorphs of 4,4'-bis(9-carbazolyl)biphenyl were prepared and characterized by X-ray diffraction and luminescence spectroscopy. Electronic structure calculations were performed to examine the influence of the molecular geometry on the HOMO and LUMO energy levels and calculated electronic transitions.

Organic electronic materials continue to see widespread use in a variety of applications including field effect transistors, photovoltaics and organic light emitting diodes (OLEDs) in large part due to the facile processing of these materials.¹⁻⁵ Many of the technologically important properties of these materials, such as the ability to conduct charge (either holes or electrons), are highly dependent on the electronic structure, energy level positions, and the supramolecular assembly of the material.⁶ While π -conjugated polymers are used in the production of high quality semiconductor thin films, molecular-based materials continue to see widespread use due to their high purity and supramolecular organization.⁷

The ability of some molecular systems to adopt two or more distinct crystal structures, polymorphism, results in functional materials with structure-dependent properties.^{8, 9} One of the most notable examples is that of pentacene, in which each of the four distinct polymorphs of pentacene exhibits differing values of charge carrier mobility, a key property for host materials in OLED applications.^{10, 11} In these applications the host material ideally suppresses quenching and triplet-triplet annihilation of the metal complex while possessing good thermal stability, high charge transport mobility and tuned triplet energies that match the corresponding emission profile for the desired OLED.¹²⁻¹⁶ One of the most widely used host materials 4,4'-bis(9-

carbazolyl)biphenyl (**CBP**) possesses a triplet energy of (2.56 eV) making **CBP** an ideal candidate for both red and green OLEDs.¹⁷

The structure of one polymorph of **CBP** (Cambridge Structural Database refcode: KANYUU) has been published by previously.^{5, 18} In this work, we report the redetermination of the

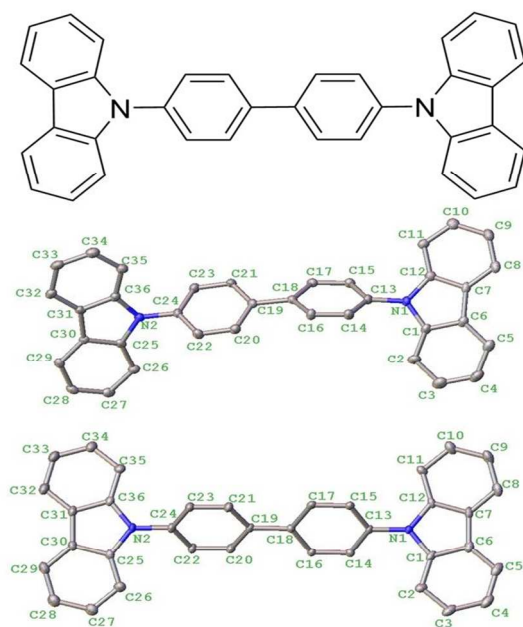


Figure 1. Chemical structure of 4,4'-bis(9-carbazolyl)biphenyl (upper) and images illustrating the thermal ellipsoids and a numbering scheme for β -CBP (middle) and γ -CBP (lower).

Table 1. Crystallographic details of the α -, β -, and γ - polymorphs of **CBP**.

Identification code	α -CBP	β -CBP	γ -CBP
Empirical formula	C ₃₆ H ₂₄ N ₂	C ₃₆ H ₂₄ N ₂	C ₃₆ H ₂₄ N ₂
Formula weight	484.57	484.57	484.57
Temperature/K	90(1)	90(1)	90(1)
Crystal system	monoclinic	orthorhombic	orthorhombic
Space group	P2 ₁ /c	Aca2	Pbca
a/Å	7.9745(18)	26.9518(17)	18.0076(10)
b/Å	16.072(4)	12.3277(8)	7.3919(4)
c/Å	10.223(3)	15.2781(10)	36.337(2)
α /°	90	90	90
β /°	110.051(7)	90	90
γ /°	90	90	90
Volume/Å ³	1230.9(5)	5076.2(6)	4836.9(5)
Z	2	8	8
ρ_{calc} mg/mm ³	1.307	1.268	1.331
μ /mm ⁻¹	0.076	0.074	0.077
F(000)	508.0	2032.0	2032.0
Crystal size/mm ³	0.2 × 0.05 × 0.02	0.2 × 0.15 × 0.05	0.25 × 0.2 × 0.05
Radiation	MoK α (λ = 0.71073 Å)	MoK α (λ = 0.71073 Å)	MoK α (λ = 0.71073 Å)
2 θ range for data collection	4.94 to 60.2°	3.02 to 54.28°	3.18 to 55.78°
Index ranges	-11 ≤ h ≤ 10, -20 ≤ k ≤ 22, -14 ≤ l ≤ 13	-34 ≤ h ≤ 34, -15 ≤ k ≤ 15, -19 ≤ l ≤ 19	-23 ≤ h ≤ 21, -9 ≤ k ≤ 9, -47 ≤ l ≤ 47
Reflections collected	13290	45931	55469
Independent reflections	3595 [R _{int} = 0.0794, R _{sigma} = 0.0776]	5621 [R _{int} = 0.0415, R _{sigma} = 0.0257]	5766 [R _{int} = 0.0912, R _{sigma} = 0.0494]
Data/restraints/parameters	3595/0/172	5621/1/343	5766/0/343
Goodness-of-fit on F ²	1.046	1.070	1.022
Final R indexes [I > 2 σ (I)]	R ₁ = 0.0496, wR ₂ = 0.1147	R ₁ = 0.0318, wR ₂ = 0.0714	R ₁ = 0.0460, wR ₂ = 0.1093
Final R indexes [all data]	R ₁ = 0.0866, wR ₂ = 0.1268	R ₁ = 0.0372, wR ₂ = 0.0737	R ₁ = 0.0660, wR ₂ = 0.1214
Largest diff. peak/hole / e Å ⁻³	0.38/-0.27	0.15/-0.18	0.24/-0.25

original structure at lower temperature and at higher resolution as well as the crystal structures of two novel polymorphs of **CBP**. The preparation of the polymorphs, their steady-state luminescence properties, and electronic structure calculations are described. While OLED layers are typically amorphous,^{19, 20} the use of polycrystalline thin films and liquid crystal layers has proven to be applicable in OLED design.²¹⁻²⁴ Thus, the existence of two new readily crystallizable **CBP** polymorphs provides engineers with two new structures and molecular orientations to consider during device design.

Results and Discussion

The previously reported polymorph of **CBP**, which will be designated α -**CBP**, was originally recrystallized from methanol at -20°C.⁵ While attempts to reproduce α -**CBP** in this manner were unsuccessful, crystals of the α -**CBP** polymorph were prepared by slow evaporation of a benzene solution of **CBP**. The first of two new polymorphs reported herein as β -**CBP** was crystallized by slow diffusion of acetone layered over a solution of **CBP** in dichloromethane for three days. The third **CBP** polymorph, γ -**CBP**, was also crystallized by slow diffusion of methanol layered upon a saturated solution of dimethylformamide (DMF).

Single crystal X-ray diffraction (SCXRD) was used to characterize all three polymorphs of **CBP**. Table 1 shows the crystallographic parameters for the three **CBP** samples. Thermal ellipsoids are also visualized along with a numbering system for the polymorphs shown in Figure 1. The packing diagrams for the three polymorphs are shown in the supplementary information. All measurements of distances and angles were performed with OLEX2.²⁵

α -CBP Polymorph

Single crystal XRD of a needle-shaped crystal grown from a benzene solution indicated that the structure was monoclinic, space group *P2₁/c*, with two formula units in the unit cell consistent with the previous report.⁵ The mean planes of the two carbazole moieties are parallel as the molecule resides on a center of symmetry. The mean plane of the biphenyl bridge linking the two groups is twisted out of plane by 49.44(4)° with respect to the mean plane of the carbazole groups as shown in Figure 2.

β -CBP Polymorph

The β polymorph crystallizes in the orthorhombic space group *Aea2* with eight formula units in the unit cell. The molecular geometry observed in this structure is markedly different from the other two polymorphs (Figure 2). The mean planes of the carbazole groups in β -**CBP** are 33.23(3)° from parallel. Likewise the mean planes of the two aromatic rings of the biphenyl group are 22.76(7)° from parallel. The aromatic rings of the biphenyl group are also twisted to a greater extent than is observed in the other polymorphs with the angles between the mean planes of the aromatic rings and the mean planes of the closest carbazole being 54.06(5)° and 65.08(5)° for the two crystallographically independent groups.

γ -CBP Polymorph

A needle-shaped crystal of γ -**CBP** analyzed by SCXRD, indicated that the structure was orthorhombic belonging to the *Pbca* space group with eight formula units in the unit cell. The

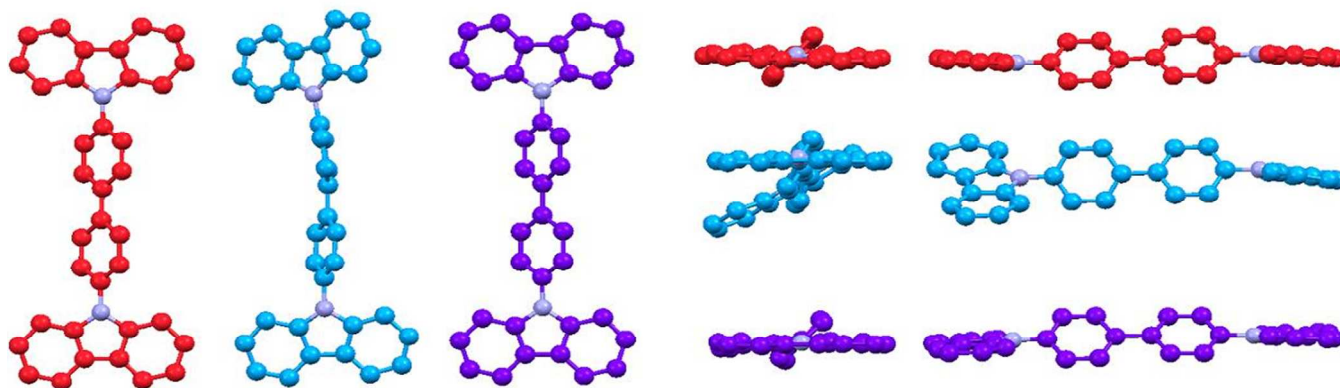


Figure 2. Ball and stick representation of α -CBP, β -CBP, and γ -CBP (red, blue, and purple respectively) illustrating the molecular geometries perpendicular to the carbazole plane (left), down the long axis of the molecules (middle) and perpendicular to both the long axis but parallel to the carbazole plane (right).

molecular geometry in this polymorph bears a strong resemblance to that of α -CBP. The two carbazole groups are nearly parallel with an angle of only $5.60(3)^\circ$ between the mean planes of the two groups. The angle between the mean planes of the neighboring crystallographically unique biphenyl and carbazole groups is $50.60(4)^\circ$ and $43.52(4)^\circ$ very similar to that of the α -polymorph.

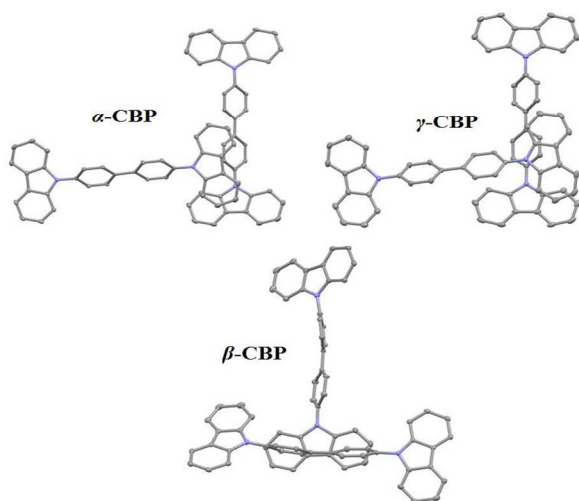


Figure 3. The close contact pairs of the three samples using two molecules from the unit cell. α -CBP and γ -CBP have similar contact pairs centered on the carbazoles, and β -CBP is closer to edge face contact between the carbazoles and the biphenyl.

Given the non-planar molecular geometries found in all three polymorphs, it is not surprising that strong π -stacking interactions are largely absent in these structures. The nearest neighbor interactions provide insight into the supramolecular crystalline organization (Figure 3). In the α - and γ -CBP structures, the long axes of neighboring pairs of molecules are approximately orthogonal with the carbazole group of one molecule overlapping a portion of the biphenyl and carbazole group of the neighbor. In β -CBP, however, a distinct edge to face interaction between the

carbazole and the biphenyl moieties of neighboring molecules is present. In all three structures, no unusually short contacts are present. All short C-H \cdots C contacts fall within the typical range of 2.6 to 2.8 Å.

Photophysical Properties

When the three crystals are irradiated with UV light and viewed under a microscope, the α - and γ -CBP polymorphs exhibit weak blue-violet emission whereas the β -CBP polymorph exhibits intense green emission. The luminescence spectra of the polymorphs following excitation using 365 nm light are shown in Figure 4. The α -CBP emission profile displays a peak at 380 nm and a less intense peak at 410 nm; two similar peaks are observed in the emission profile of γ -CBP. The similarity of the emission spectra for these two polymorphs is not surprising given the similarities of the molecular geometry observed for these two polymorphs. The emission spectrum of β -CBP is broad and featureless at wavelengths below 450 nm. A large

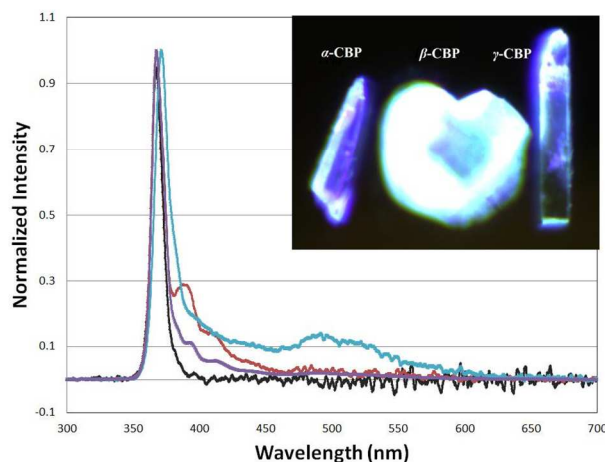


Figure 4. A graph showing the normalized emission profiles of α -CBP, β -CBP, and γ -CBP (red, blue, and purple respectively) along with a visual comparison of the three crystals under UV light irradiation. The strong peak at 365 nm is scattering from the excitation source (black).

broad peak at approximately 500 nm is responsible for the observed green luminescence from this polymorph (Figure 4).

Theoretical Calculations

To help understand the impact of the observed geometries on the electronic structure of the molecules, molecular orbitals and UV/Visible spectra were calculated using DFT and TD-DFT methods, respectively. Gas phase calculations were performed on the three unique molecular geometries determined from XRD on the three polymorphs. Shown in Figure 5 are the highest occupied molecular orbitals (HOMO) and lowest unoccupied molecular orbitals (LUMO) for the three **CBP** molecules. The HOMOs of these three samples appear to be distributed over the entire molecule with major contributions from the nitrogen p atomic orbitals. The LUMOs of these molecules are composed entirely of atomic orbitals of the biphenyl moieties.

The calculated HOMO-LUMO gaps, ΔE , are 3.891 eV, 3.993 eV, and 3.925 eV for the α -**CBP**, β -**CBP** and γ -**CBP** polymorphs respectively. While the HOMO-LUMO gap of the two similar polymorphs differs by only 34 meV, the gap of the β -polymorph is over 100 meV larger than that of α -**CBP**.

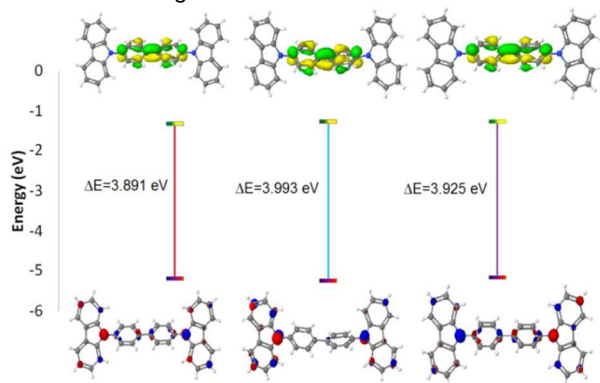


Figure 5. Energy level diagram featuring the HOMO-LUMO molecular orbitals and energy gap for the states of the α -**CBP** (left), β -**CBP** (middle), and γ -**CBP** (right) polymorphs. Isosurface ± 0.05 a.u.

That β -**CBP** possesses the highest HOMO-LUMO gap is somewhat expected as the pronounced distortions in this molecule will disrupt the conjugation of the molecule and thereby raise the energy of the HOMO-LUMO gap. However, the larger HOMO-LUMO gap relative to the gap of other two geometries should result in higher energy emission whereas the opposite is observed. It is well-documented that purely organic crystalline systems are capable of phosphorescent emission.²⁶⁻²⁸ The observed green emission in this polymorph may arise from intramolecular contacts not present in the other two polymorphs.

Conclusions

Designing materials with tailor-made properties requires an in-depth understanding of the influence of molecular structure on the physical properties of the system. In the present study, three polymorphs of the electro-optic material **CBP** have been successfully grown and structurally and spectroscopically characterized. The two geometrically similar polymorphs, α -**CBP** and γ -**CBP**, possess similar electronic structures and emission

profiles. The larger HOMO-LUMO gap of β -**CBP** combined with the observed low energy emission of this crystalline form indicates that packing features present in this polymorph may play an important role in the emission characteristics for this crystalline phase.

Experimental

Sample preparation

The powdered form of 4,4'-bis(9-carbazolyl)biphenyl (97% pure) was purchased from Sigma-Aldrich and used without further purification. Crystallizations were performed using slow solvent evaporations on 15 mg samples. α -**CBP** was crystallized using 3mL of benzene over a 3 day period. β -**CBP** was crystallized by slow diffusion of acetone layered over a solution of **CBP** in dichloromethane for three days. γ -**CBP** was crystallized by slow diffusion of methanol layered upon a saturated solution of dimethylformamide over 20 days.

Single-crystal X-ray diffraction

Crystals suitable for X-ray diffraction were selected and mounted on a glass capillary with oil. X-ray diffraction data for all samples was collected using a Bruker SMART APEX2 CCD diffractometer installed at a rotating anode source (MoK α radiation, $\lambda=0.71073$ Å), and equipped with an Oxford Cryosystems (Cryostream 700) nitrogen gas-flow apparatus. The data was collected by the rotation method with 0.5° frame-width (ω scan) and exposure time per frame varied for each sample. Generally five sets of data (360 frames in each set) were collected for each compound, nominally covering complete reciprocal space. The crystals were kept at 90 K during data collection. The determination of unit cell parameters and the integration of raw diffraction images were performed with the APEX2 program package.²⁹ Using Olex2,²⁵ the structures were solved with the ShelXS structure solution program using direct methods and refined with the ShelXL refinement package using Least Squares minimization.³⁰ The structures were refined by full matrix least squares against F^2 .

Photophysical measurements

Single crystals were mounted on a quartz slide using low-fluorescence immersion oil and centered on a luminescence microscope in which the emission of an irradiated sample is collected using a 15x reflecting objective (Newport Model 50105-02), transferred to a fiber optic (Thorlabs FT030 - Orange Reinforced 3.0 mm furcation tubing) where the intensity is subsequently analyzed using a Miniature Fiber Optic Spectrometer (Ocean Optics USB4000-UV-VIS). The samples were irradiated using the focused output of a high-power LED source (Thor Labs, typical optical LED output power <360 mW, 365 nm).

Theoretical calculations

Density functional theory (DFT) calculations on the experimental structures of **CBP** were performed with the Gaussian 09 program

package³¹ using the WebMO interface.³² The hybrid exchange correlation functional B3LYP was used for all of the calculations in the present study. Final calculations were completed using the 6-31G(d,p) basis set.

Notes and references

^a Department of Chemistry, University at Buffalo, The State University of New York, Buffalo, NY 14260-3000, U.S.A.

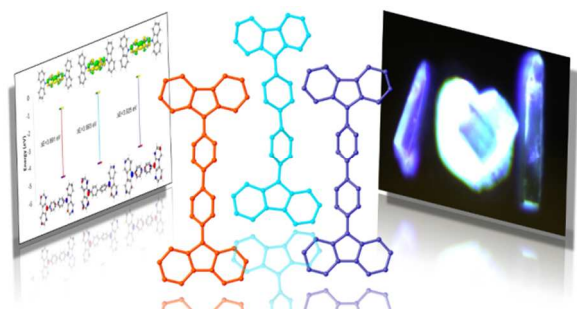
Electronic Supplementary Information (ESI) available: Full reference for reference 31, crystal packing diagrams, and additional crystallographic information tables. See DOI: 10.1039/c000000x/

The authors declare no competing financial interests.

Acknowledgment: Partial support of this work was provided by the University at Buffalo, The State University of New York.

References:

1. T. T. Steckler, X. Zhang, J. Hwang, R. Honeyager, S. Ohira, X.-H. Zhang, A. Grant, S. Ellinger, S. A. Odom, D. Sweat, D. B. Tanner, A. G. Rinzler, S. Barlow, J.-L. Bredas, B. Kippelen, S. R. Marder and J. R. Reynolds, *J. Am. Chem. Soc.*, 2009, **131**, 2824-2826.
2. T. Kono, D. Kumaki, J. Nishida, S. Tokito and Y. Yamashita, *Chem. Commun. (Cambridge, U. K.)*, 2010, **46**, 3265-3267.
3. T. Hasegawa and J. Takeya, *Science and Technology of Advanced Materials*, 2009, **10**.
4. M. O'Neill and S. M. Kelly, *Adv. Mater. (Weinheim, Ger.)*, 2003, **15**, 1135-1146.
5. P. J. Low, M. A. J. Paterson, D. S. Yufit, J. A. K. Howard, J. C. Cherryman, D. R. Tackley, R. Brook and B. Brown, *J. Mater. Chem.*, 2005, **15**, 2304-2315.
6. M. Mas-Torrent and C. Rovira, *Chem. Rev.*, 2011, **111**, 4833-4856.
7. F. J. M. Hoeben, P. Jonkheijm, E. W. Meijer and A. Schenning, *Chem. Rev.*, 2005, **105**, 1491-1546.
8. M. A. Baldo, D. F. O'Brien, Y. You, A. Shoustikov, S. Sibley, M. E. Thompson and S. R. Forrest, *Nature*, 1998, **395**, 151-154.
9. D. E. Cohen, J. B. Benedict, B. Morlan, D. T. Chiu and B. Kahr, *Cryst. Growth Des.*, 2007, **7**, 492-495.
10. C. Adachi, M. A. Baldo, M. E. Thompson and S. R. Forrest, *J. Appl. Phys.*, 2001, **90**, 5048-5051.
11. A. G. Dikundwar, G. K. Dutta, T. N. Guru Row and S. Patil, *Cryst. Growth Des.*, 2011, **11**, 1615-1622.
12. M. Irie, *Photochem. Photobiol. Sci.*, 2010, **9**, 1535-1542.
13. J. He, T. Wang, S. Chen, R. Zheng, H. Chen, J. Li and H. Zeng, *Journal of Photochemistry and Photobiology A: Chemistry*, 2014, **277**, 45-52.
14. T. Zhang, Y. Liang, J. Cheng and J. Li, *Journal of Materials Chemistry C*, 2013, **1**, 757-764.
15. T. Nakagawa, S.-Y. Ku, K.-T. Wong and C. Adachi, *Chem. Commun. (Cambridge, U. K.)*, 2012, **48**, 9580-9582.
16. V. V. Cherpak, P. Y. Stakhira, D. Y. Volyniuk, J. Simokaitiene, A. Tomkeviciene, J. V. Grazulevicius, A. Bucinskas, V. M. Yashchuk, A. V. Kukhta, I. N. Kukhta, V. V. Kosach and Z. Y. Hotra, *Synth. Met.*, 2011, **161**, 1343-1346.
17. C.-L. Ho, L.-C. Chi, W.-Y. Hung, W.-J. Chen, Y.-C. Lin, H. Wu, E. Mondal, G.-J. Zhou, K.-T. Wong and W.-Y. Wong, *J. Mater. Chem.*, 2012, **22**, 215-224.
18. F. Allen, *Acta Crystallographica Section B*, 2002, **58**, 380-388.
19. K. Goushi, R. Kwong, J. J. Brown, H. Sasabe and C. Adachi, *J. Appl. Phys.*, 2004, **95**, 7798-7802.
20. D. F. O'Brien, M. A. Baldo, M. E. Thompson and S. R. Forrest, *Appl. Phys. Lett.*, 1999, **74**, 442-444.
21. Z. B. Wang, M. G. Helander, QiuJ, D. P. Puzzo, M. T. Greiner, Z. M. Hudson, WangS, Z. W. Liu and Z. H. Lu, *Nat Photon*, 2011, **5**, 753-757.
22. X. Zhou, M. Pfeiffer, J. Blochwitz, A. Werner, A. Nollau, T. Fritz and K. Leo, *Appl. Phys. Lett.*, 2001, **78**, 410-412.
23. W. Pisula, M. Zorn, J. Y. Chang, K. Müllen and R. Zentel, *Macromol. Rapid Commun.*, 2009, **30**, 1179-1202.
24. P. Brulatti, V. Fattori, S. Muzzioli, S. Stagni, P. P. Mazzeo, D. Braga, L. Maini, S. Milita and M. Cocchi, *Journal of Materials Chemistry C*, 2013, **1**, 1823-1831.
25. O. V. Dolomanov, L. J. Bourhis, R. J. Gildea, J. A. K. Howard and H. Puschmann, *J. Appl. Crystallogr.*, 2009, **42**, 339-341.
26. J. Xu, A. Takai, Y. Kobayashi and M. Takeuchi, *Chem. Commun. (Cambridge, U. K.)*, 2013, **49**, 8447-8449.
27. W. Z. Yuan, X. Y. Shen, H. Zhao, J. W. Y. Lam, L. Tang, P. Lu, C. Wang, Y. Liu, Z. Wang, Q. Zheng, J. Z. Sun, Y. Ma and B. Z. Tang, *The Journal of Physical Chemistry C*, 2010, **114**, 6090-6099.
28. O. Bolton, K. Lee, H.-J. Kim, K. Y. Lin and J. Kim, *Nat Chem*, 2011, **3**, 205-210.
29. G. M. Sheldrick, *SADABS*, (2004), Universität Göttingen, Germany.
30. G. Sheldrick, *Acta Crystallographica Section A*, 2008, **64**, 112-122.
31. M. J. Frisch, et al., *Gaussian 09, Revision A.02*, (2009), Wallingford CT.
32. J. R. Schmidt and W. F. Polik, *WebMO Enterprise*, (2013) WebMO LLC, Holland, MI USA.



TOC: Single crystal structures, luminescent properties and electronic structure calculations of three polymorphs of the opto-electronic charge transport material 4,4'-bis(9-carbazolyl)biphenyl